


Article

Spaceborne Estimation of Leaf Area Index in Cotton, Tomato, and Wheat Using Sentinel-2

Gregoriy Kaplan  and Offer Rozenstein *

Institute of Soil, Water and Environmental Sciences, Agricultural Research Organization-Volcani Institute, HaMaccabim Road 68, P.O.B 15159, Rishon LeZion 7528809, Israel; grigorii@volcani.agri.gov.il

* Correspondence: offerr@volcani.agri.gov.il

Abstract: Satellite remote sensing is a useful tool for estimating crop variables, particularly Leaf Area Index (LAI), which plays a pivotal role in monitoring crop development. The goal of this study was to identify the optimal Sentinel-2 bands for LAI estimation and to derive Vegetation Indices (VI) that are well correlated with LAI. Linear regression models between time series of Sentinel-2 imagery and field-measured LAI showed that Sentinel-2 Band-8A—Narrow Near InfraRed (NIR) is more accurate for LAI estimation than the traditionally used Band-8 (NIR). Band-5 (Red edge-1) showed the lowest performance out of all red edge bands in tomato and cotton. A novel finding was that Band 9 (Water vapor) showed a very high correlation with LAI. Bands 1, 2, 3, 4, 5, 11, and 12 were saturated at $LAI \approx 3$ in cotton and tomato. Bands 6, 7, 8, 8A, and 9 were not saturated at high LAI values in cotton and tomato. The tomato, cotton, and wheat LAI estimation performance of reNDVI ($R^2 = 0.79, 0.98, 0.83$, respectively) and two new VIs (WEVI (Water vapor red Edge Vegetation Index) ($R^2 = 0.81, 0.96, 0.71$, respectively) and WNEVI (Water vapor narrow NIR red Edge Vegetation index) ($R^2 = 0.79, 0.98, 0.79$, respectively)) were higher than the LAI estimation performance of the commonly used NDVI ($R^2 = 0.66, 0.83, 0.05$, respectively) and other common VIs tested in this study. Consequently, reNDVI, WEVI, and WNEVI can facilitate more accurate agricultural monitoring than traditional VIs.

Keywords: Sentinel-2; spectral bands; LAI; vegetation indices



Citation: Kaplan, G.; Rozenstein, O. Spaceborne Estimation of Leaf Area Index in Cotton, Tomato, and Wheat Using Sentinel-2. *Land* **2021**, *10*, 505. <https://doi.org/10.3390/land10050505>

Academic Editor: Javier Cabello

Received: 26 March 2021

Accepted: 7 May 2021

Published: 9 May 2021

Publisher's Note: MDPI stays neutral with regard to jurisdictional claims in published maps and institutional affiliations.



Copyright: © 2021 by the authors. Licensee MDPI, Basel, Switzerland. This article is an open access article distributed under the terms and conditions of the Creative Commons Attribution (CC BY) license (<https://creativecommons.org/licenses/by/4.0/>).

1. Introduction

Monitoring crop growth and performance during developmental stages is an essential aspect of agricultural management. Leaf Area Index (LAI) is a good proxy of the vegetation state [1–3] and a good yield predictor [4–6]. LAI is a dimensionless quantity that characterizes plant canopies. It is defined as the one-sided green leaf area per unit ground surface area. The LAI is an important parameter in plant ecology and a measure of the photosynthetic active area, and at the same time of the area subjected to transpiration. It is also the area that comes in contact with air pollutants. LAI is often a key biophysical variable used in biogeochemical, hydrological, and ecological models. LAI is also commonly used as a measure of crop growth and productivity at spatial scales ranging from the plot to the globe. Moreover, activities such as herbicide and fertiliser management, leaf chlorophyll content estimation, detection of crop disease, and yield prediction can be based on LAI monitoring [7].

LAI can be estimated from VIs [8–11] produced from imagery acquired by optical satellites, but this approach suffers from a low correlation between LAI and some bands that the VIs are based on. Many studies showed that LAI estimation from optical imagery suffers from saturation when LAI is greater than 3 (i.e., the LAI changes at a faster rate than the reflectance) [11–14]. Since the LAI of many crops typically exceeds this level by a large margin, optical sensors have limited use for LAI estimation. Most previous studies that defined this saturation effect were based on older sensors (e.g., Landsat, Modis, SPOT) [15–17], and accordingly, Vegetation Indices (VIs) intended for those sensors. In 2015

the first Sentinel-2 became operational, which marked the arrival of the new generation of satellites. The Multi-Spectral Instrument (MSI) onboard Sentinel-2 observes the earth at 13 spectral bands with a spatial resolution from 10 to 60 m (depending on the band) and a five-day revisit time. MSI is a spaceborne multispectral instrument that thoroughly covers the red edge spectral range, which is highly sensitive to the chlorophyll reflectance in plants [18]. The red-edge spectral range covers the wavelengths of 680–750 nm, where the change of leaf reflectance is sharp [19,20]. In order to estimate LAI from Sentinel-2, there is a need to evaluate which bands suffer from the saturation that was observed in previous generations of spaceborne sensors and explore ways to overcome this limitation.

In addition to LAI modelling based on VIs, several machine learning algorithms for LAI estimation based on Sentinel-2 bands were studied and showed mixed results [11,21–23]. Previous studies on different wavebands [24], including simulated Sentinel-2 bands, concluded that the red edge is the best spectral region for LAI estimation in several crops [2,3,25–27]. Therefore, careful selection of the bands used to derive VIs and machine learning algorithms can improve the performance and generality of the LAI estimation models based on Sentinel-2 imagery. Nevertheless, while several studies investigated the performance of MSI-based VIs and machine learning algorithms for LAI estimation of tomato, wheat, and cotton [11,28–30], very few studies investigated the performance of the real MSI bands (as opposed to synthetic data) in the LAI estimation of these crops [31].

Therefore, this study's first goal was to model LAI using real Sentinel-2 imagery and field-measured LAI to quantify the performance of individual bands and their saturation levels in cotton, tomato and wheat. The second goal of the study was to suggest well-performing VIs that employ bands not commonly used for VI derivation and facilitate better agricultural monitoring.

2. Materials and Methods

2.1. Test Sites and Field Measurements

The field data used in this study were collected during one cotton, two wheat, and three processing tomatoes experiments conducted in five locations in Israel (Figure 1).

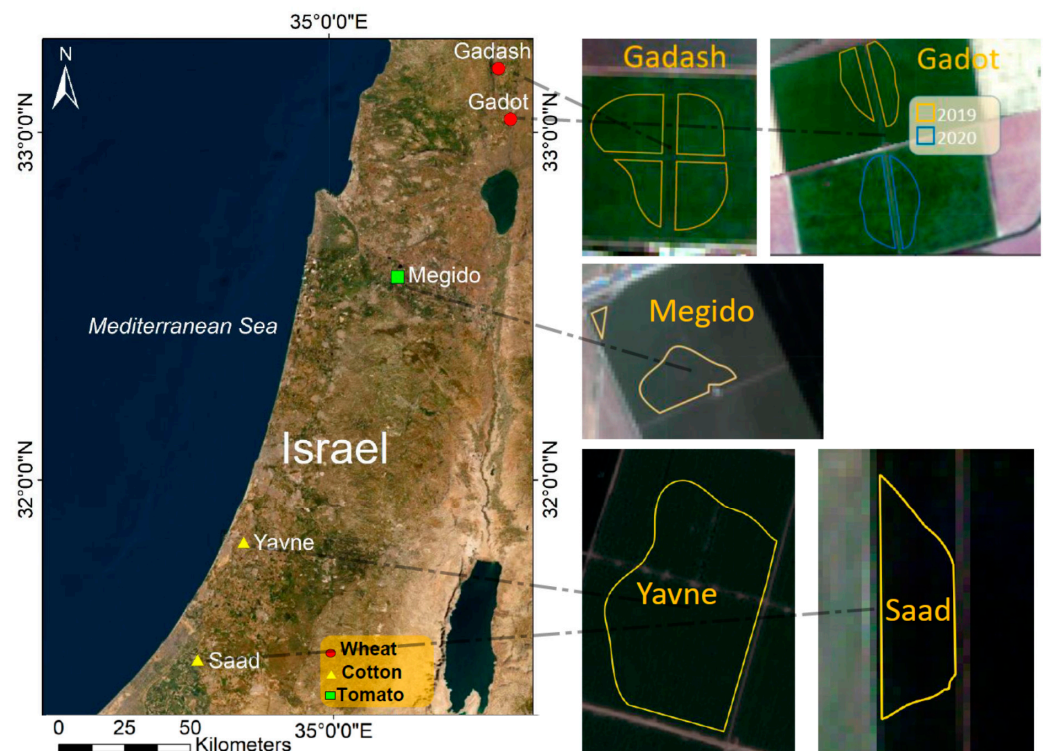


Figure 1. Locations and analysis polygons of the experiments conducted in Israel in 2018–2020.

The Sentinel-2 image inventory used for this study is presented in Table 1. Overall, 56 Sentinel-2 images were used in the study (14—wheat, 33—processing tomatoes, 9—cotton). During these experiments, LAI was measured by a SunScan Canopy Analysis System—SS1 developed by Delta-T Company (Cambridge, United Kingdom). The SunScan is a widely used, accurate, nondestructive LAI measurement system successfully employed in many previous studies [5,30,32]. The SunScan system measures LAI by calculating the difference in solar radiance received by the dome sensor installed under unobscured Sun view and the hand-held probe placed below vegetation canopy on the ground level (Figure 2).

Table 1. The Sentinel-2 bands used in the present study.

| Band | Sentinel-2A | | Sentinel-2B | | Spatial Resolution (m) |
|------------------------------|-------------------------|----------------|-------------------------|----------------|------------------------|
| | Central Wavelength (nm) | Bandwidth (nm) | Central Wavelength (nm) | Bandwidth (nm) | |
| Band 1—Coastal aerosol | 442.7 | 21 | 442.2 | 21 | 60 |
| Band 2—Blue | 492.4 | 66 | 492.1 | 66 | 10 |
| Band 3—Green | 559.8 | 36 | 559.0 | 36 | 10 |
| Band 4—Red | 664.6 | 31 | 664.9 | 31 | 10 |
| Band 5—Vegetation red edge 1 | 704.1 | 15 | 703.8 | 16 | 20 |
| Band 6—Vegetation red edge 1 | 740.5 | 15 | 739.1 | 15 | 20 |
| Band 7—Vegetation red edge 3 | 782.8 | 20 | 779.7 | 20 | 20 |
| Band 8—NIR | 832.8 | 106 | 832.9 | 106 | 10 |
| Band 8A—Narrow NIR | 864.7 | 21 | 864.0 | 22 | 20 |
| Band 9—Water vapour | 945.1 | 20 | 943.2 | 21 | 60 |
| Band 11—SWIR | 1613.7 | 91 | 1610.4 | 94 | 20 |
| Band 12—SWIR | 2202.4 | 175 | 2185.7 | 185 | 20 |



Figure 2. Main components of the SunScan system: (A) Dome sensor; (B) Probe; (C) Field computer.

Each LAI value used for model calibration was an average value of at least 30 field measurements. LAI was measured in the center of the fields and was correlated to average values of Sentinel-2 bands and VIs of homogenous areas in the fields' centers. In the Megido 2020 experiment, LAI was measured in two areas of the field (in the center of the field (six LAI measurements) and on the northwest corner (four LAI measurements)) where the crop developed at different rates and, thus, LAI was different. Accordingly, both time series of the field measurements were correlated with the average values of bands and VIs within defined polygons. In-field paths and their surrounding area were masked out from analysis polygons of the tomato experiments to remove bare soil areas and avoid border effects. These excluded areas consisted of approximately 20% of the overall polygon areas in the tomato fields. Therefore, each tomato polygon consisted of either two or four vegetated regions separated by the paths.

Overall, 11 averaged LAI values taken during two growing seasons were used for deriving the wheat models, nine for cotton (one season), and 23 for tomato (three seasons).

The linear regression models in this study utilised the average values derived from satellite imagery within the analysis polygons and same-date field measurements or linearly interpolated LAI values of field measurements from adjacent dates.

2.2. Satellite Imagery

Sentinel-2 is an Earth observation mission and part of the European Space Agency (ESA) Copernicus program. It includes two satellites with a payload of MSI, namely Sentinel-2A (launched 23 June 2015) and Sentinel-2B (launched 7 March 2017). Table 1 lists the spectral bands of Sentinel-2 that were used in this study. The inventory of the atmospherically and topographically corrected Level-2A Sentinel-2 images used in this study alongside the information on the LAI measurements can be found in Tables 2 and A1. Level-2A and Level-1C imagery were downloaded from the ESA Copernicus site (<https://scihub.copernicus.eu/dhus/#/home>, accessed on 6 April 2021) (# means “Number”). Level-1C images were processed to Level-2A using Sen2Cor algorithm [33].

Table 2. Sentinel-2 imagery and LAI measurements used in the study.

| Area | Crop | Period * | # of Images | Polygon Size (Sentinel-2 Pixels) | # LAI Measurements | Range of Measured LAI |
|--------|--------|----------------------------------|-------------|----------------------------------|--------------------|-----------------------|
| Saad | Wheat | 02-March-2019 06-April-2019 | 6 | 260 | 4 | 4.8–7.1 |
| Yavne | Wheat | 11-January-2019 11-April-2019 | 8 | 550 | 7 | 3.8–7.0 |
| Gadash | Tomato | 3-May-2019 24-July-2019 | 8–9 ** | 425 | 6 | 1.4–4.7 |
| Gadot | Tomato | 25-April-2019 14-August-2019 | 12–13 ** | 249 | 11 | 0.7–9.1 |
| Gadot | Tomato | 7-May-2020 3-August-2020 | 11 | 332 | 6 | 0.9–8.6 |
| Megido | Cotton | 30-May-2020 | 9 | 268 (Centre) | 6 | 0.6–9.6 |
| | | 29-July-2020 | 4 | 17 (NW Corner) | 3 | 0.8–1.9 |

* Indicates the dates of the first and last images. ** A defective red edge band in a Sentinel-2 image acquired on 10 June 2019 prevented the derivation of red edge-based models for that date.

2.3. Model Calibration and Validation

Linear regression models were derived to estimate LAI for specific crops based on field measurements and Sentinel-2 bands. Similarly, regression models between LAI and VIs were derived, including NDVI [34] and NDVI based on the Narrow NIR Band-8A instead of NIR Band-8. Additionally to NDVI, models were also derived for reNDVI [35], MTCI [36], WDVI [37], EVI [38], SAVI [39], MSAVI [40], DVI [34], and two new indices: WEVI (Water vapor red Edge Vegetation Index) and WNEVI (Water vapor narrow NIR red Edge Vegetation index). For every model, the R^2 and root mean square error (RMSE) values were calculated using the Microsoft Excel software. WEVI and WNEVI were developed based on combinations of the best performing bands for LAI estimation. The following equations and Sentinel-2 bands were used for deriving the aforementioned VIs:

$$\text{NDVI} = (\text{B8} - \text{B4}) / (\text{B8} + \text{B4}) \quad (1)$$

$$\text{NDVI8A} = (\text{B8A} - \text{B4}) / (\text{B8A} + \text{B4}) \quad (2)$$

$$\text{MTCI} = (\text{B6} - \text{B5}) / (\text{B5} - \text{B4}) \quad (3)$$

$$\text{WDVI} = \text{B8} - 0.5 \times \text{B4} \quad (4)$$

$$\text{EVI} = (2.5 \times (\text{B8} - \text{B4})) / (\text{B8} + 6 \times \text{B4} - 7.5 \times \text{B2} + 1) \quad (5)$$

$$\text{SAVI} = ((\text{B8} - \text{B4})) / (\text{B8} + \text{B4} + 0.5)) \times 1.5 \quad (6)$$

$$\text{MSAVI} = ((\text{B8} - \text{B4}) \times (1 + \text{L})) / (\text{B8} + \text{B4} + \text{L}) \quad (7)$$

where: $L = 1 - 2 \times s \times NDVI \times WdVI$ and s is the soil line slope = 0.5

$$DVI = B8 - B4 \quad (8)$$

$$reNDVI = (B8A - B6)/(B8A + B6) \quad (9)$$

$$WEVI = B9 - B6 \quad (10)$$

$$WNEVI = (B8A - B6)/(B9 + B6) \quad (11)$$

3. Results

Table 3 shows the performance of the separate Sentinel-2 bands and VIs for LAI estimation of cotton, tomato, and wheat. Overall, the bands that modelled LAI best were Band-7 (Red edge-3), Band-9 (Water vapor), and two NIR bands (8 and 8A). Notably, Band-8A (Narrow NIR) showed a higher correlation with LAI and lower RMSE in LAI estimation than Band-8 (NIR) in all three crops. Consequently, NDVI8A performed better than NDVI. Importantly, Band-4 (Red) showed average performance, and Band-5 (Red edge-1) showed weak performance relative to other bands in tomato and cotton. Therefore VIs based on the better performing bands might be beneficial for LAI estimation. One such VI, namely reNDVI, showed a very high estimation performance. Finally, the high performance in LAI prediction by the Water vapor Band-9 suggests that this band might be useful for creating VIs with good correlation to LAI. This result was confirmed by low RMSE and high R^2 values of the new WEVI and WNEVI that are based on Band-9. The two new VIs proposed in the study (WEVI and WNEVI) alongside reNDVI showed superior performance in LAI predictions compared to NDVI and NDVI8A in all three crops, with the largest difference in wheat.

Table 3. Performance of Sentinel-2 bands and VIs used in the present study. The performance of best performing bands and VIs for each crop are in bold.

| Band/VI | Tomato | | Cotton | | Wheat | |
|----------------------------|-------------|------------|-------------|------------|-------------|------------|
| | R^2 | RMSE | R^2 | RMSE | R^2 | RMSE |
| Band 1—Coastal aerosol | 0.08 | 2.4 | 0.58 | 2.4 | 0.17 | 1.1 |
| Band 2—Blue | 0.13 | 2.3 | 0.52 | 2.5 | 0.02 | 1.2 |
| Band 3—Green | 0.00 | 2.5 | 0.57 | 2.4 | 0.06 | 1.2 |
| Band 4—Red | 0.65 | 1.5 | 0.81 | 1.6 | 0.02 | 1.2 |
| Band 5—Vegetation red edge | 0.00 | 2.5 | 0.75 | 1.8 | 0.22 | 1.1 |
| Band 6—Vegetation red edge | 0.79 | 1.1 | 0.93 | 1.0 | 0.01 | 1.2 |
| Band 7—Vegetation red edge | 0.78 | 1.2 | 0.96 | 0.7 | 0.26 | 1.0 |
| Band 8—NIR | 0.78 | 1.2 | 0.96 | 0.7 | 0.23 | 1.1 |
| Band 8A—Narrow NIR | 0.82 | 1.1 | 0.97 | 0.7 | 0.34 | 1.0 |
| Band 9—Water vapour | 0.80 | 1.1 | 0.97 | 0.7 | 0.29 | 1.0 |
| Band 11—SWIR | 0.01 | 2.5 | 0.12 | 3.4 | 0.00 | 1.2 |
| Band 12—SWIR | 0.61 | 1.6 | 0.82 | 1.5 | 0.00 | 1.2 |
| NDVI | 0.66 | 1.4 | 0.83 | 1.5 | 0.05 | 1.2 |
| NDVI8A | 0.71 | 1.3 | 0.87 | 1.3 | 0.05 | 1.2 |
| reNDVI | 0.79 | 1.1 | 0.98 | 0.6 | 0.83 | 0.5 |
| MTCI | 0.16 | 2.3 | 0.95 | 0.8 | 0.53 | 0.8 |
| WDVI | 0.76 | 1.2 | 0.94 | 0.9 | 0.29 | 1.0 |
| EVI | 0.78 | 1.2 | 0.95 | 0.8 | 0.26 | 1.0 |
| SAVI | 0.73 | 1.3 | 0.92 | 1.0 | 0.14 | 1.1 |
| MSAVI | 0.75 | 1.2 | 0.93 | 1.0 | 0.15 | 1.5 |
| DVI | 0.77 | 1.2 | 0.94 | 0.9 | 0.19 | 1.1 |
| WEVI | 0.81 | 1.1 | 0.96 | 0.7 | 0.71 | 0.6 |
| WNEVI | 0.79 | 1.1 | 0.98 | 0.6 | 0.79 | 0.5 |

Figure 3 shows the reflectance in each band and the corresponding LAI measurements in this study's experiments. The reflectance in bands 1, 2, 3, 4, 5, 11, 12 in cotton and processing tomatoes start saturating from $LAI \approx 3$ and almost no longer changing at

LAI \approx 6. This result is especially important because bands 4 and 5 are used in many VIs. On the other hand, bands 6, 7, 8, 8A, 9 were not saturated. Insufficient satellite imagery and field measurements of LAI were acquired during the wheat experiments and hindered estimating the saturation levels of this crop.

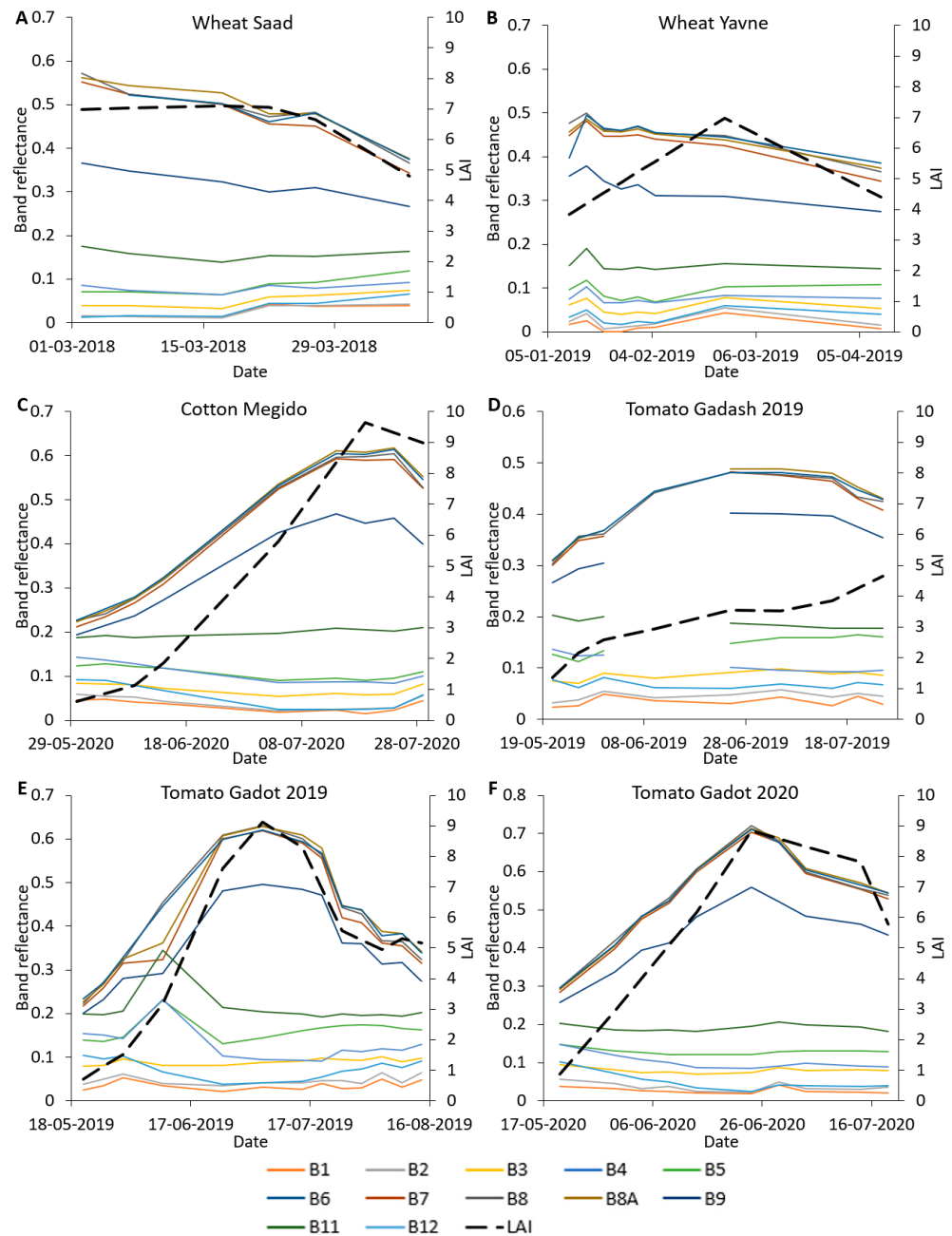


Figure 3. Band reflectance and LAI measurements in the following experiments: (A) Wheat Saad, (B) Wheat Yavne, (C) Cotton Megido (centre of field), (D) Tomato Gadash 2019, (E) Tomato Gadot 2019, (F) Tomato Gadot 2020.

Figure 4 shows the RMSE of Sentinel-2 bands LAI estimation for wheat, cotton, and tomato. While the RMSE of Sentinel-2 bands most commonly used in VIs formulae (bands 2-8A) in wheat LAI estimation is closer to each other, Band-4 and Band-5 have notably high RMSE in cotton and tomato LAI estimation, and this is especially pronounced for Band-5 in tomato.

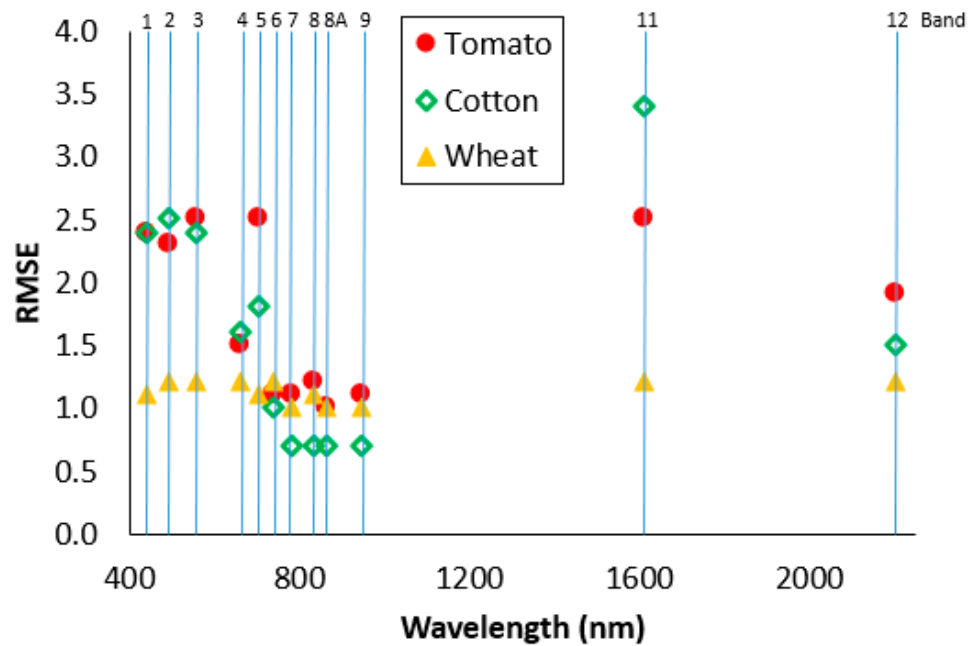


Figure 4. RMSE of Sentinel-2 bands in tomato, cotton, and wheat LAI estimation.

Figure 5 shows reNDVI, WEVI, WNEVI, NDVI, and MTCI linear regression models for tomato, cotton, and wheat.

Figure 6 shows the LAI measurements and LAI estimation based on the VIs used in this study using the models described in Table 3. While several VIs showed similar behavior in LAI estimation, MTCI, MSAVI, reNDVI, WEVI, and WNEVI were notably different. MTCI, affected by the low performance of the Band-5, did not perform well in tomato LAI estimation in Gadot 2019 and 2020. MSAVI notably underestimated wheat LAI values. Conversely, reNDVI, WEVI, and WNEVI show closer resemblance to measured LAI than all other VIs. In the present study, no difference in the spectral response of Sentinel-2A and -B satellites was observed owing to an excellent radiometric cross-calibration of the MSI on both satellites.

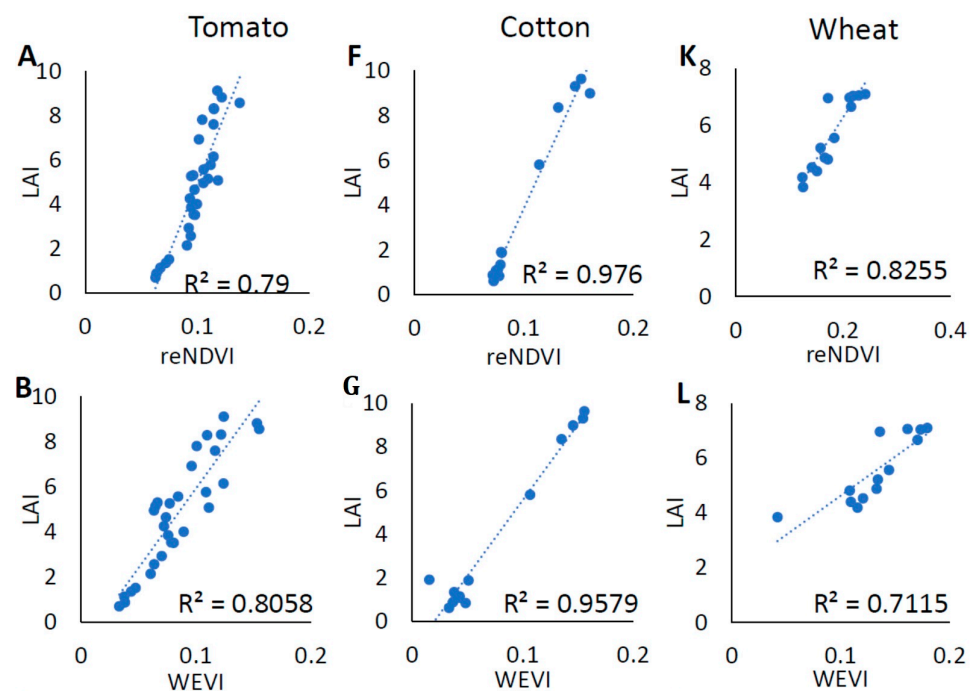


Figure 5. Cont.

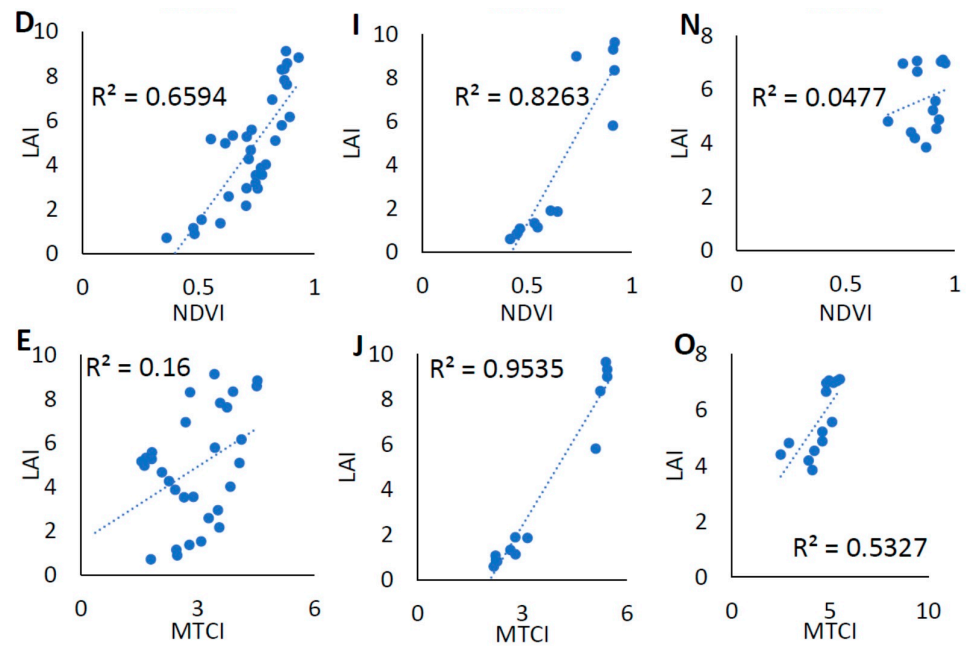


Figure 5. Tomato, cotton, and wheat LAI-VI linear regression models: (A) Tomato reNDVI; (B) Tomato WEVI; (C) Tomato WNEVI; (D) Tomato NDVI; (E) Tomato MTCI; (F) Cotton reNDVI; (G) Cotton WEVI; (H) Cotton WNEVI; (I) Cotton NDVI; (J) Cotton MTCI; (K) Wheat reNDVI; (L) Wheat WEVI; (M) Wheat WNEVI; (N) Wheat NDVI; (O) Wheat MTCI. The data used to derive the models is presented in Table 2, the RMSE values of the models are given in Table 3.

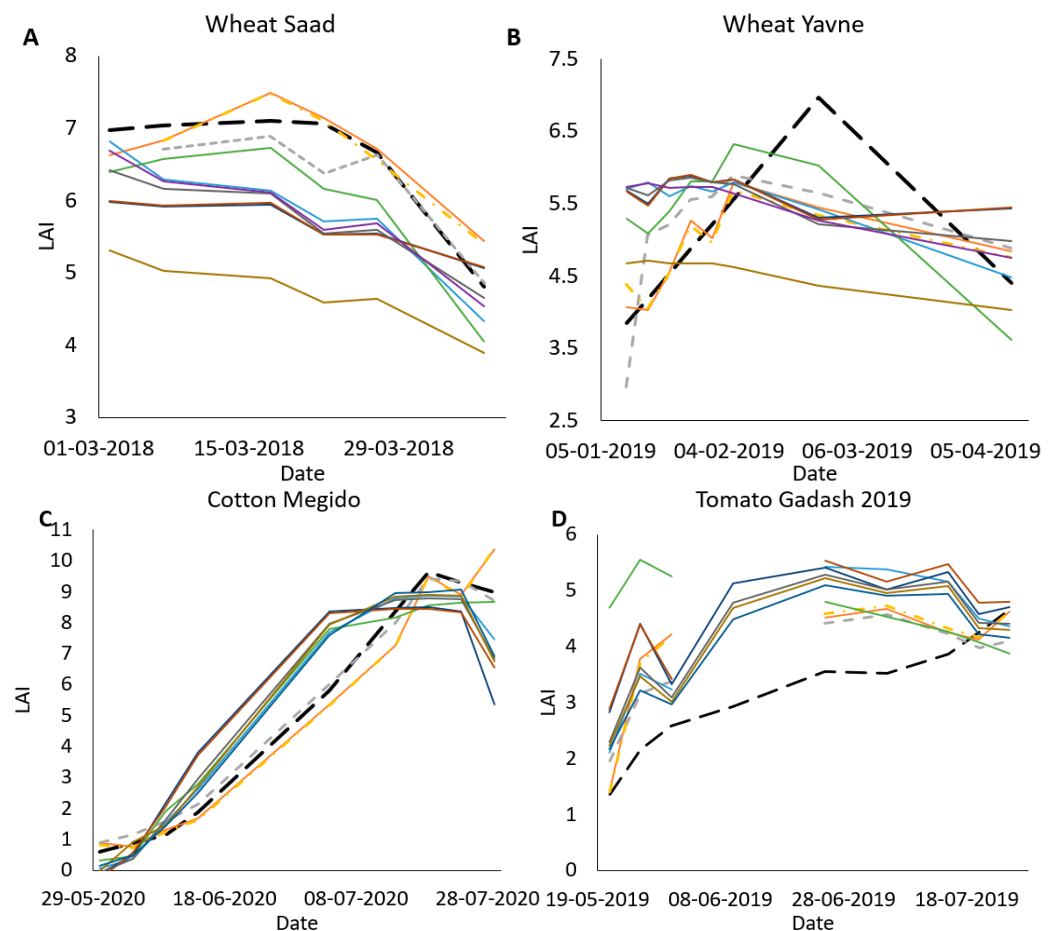


Figure 6. Cont.

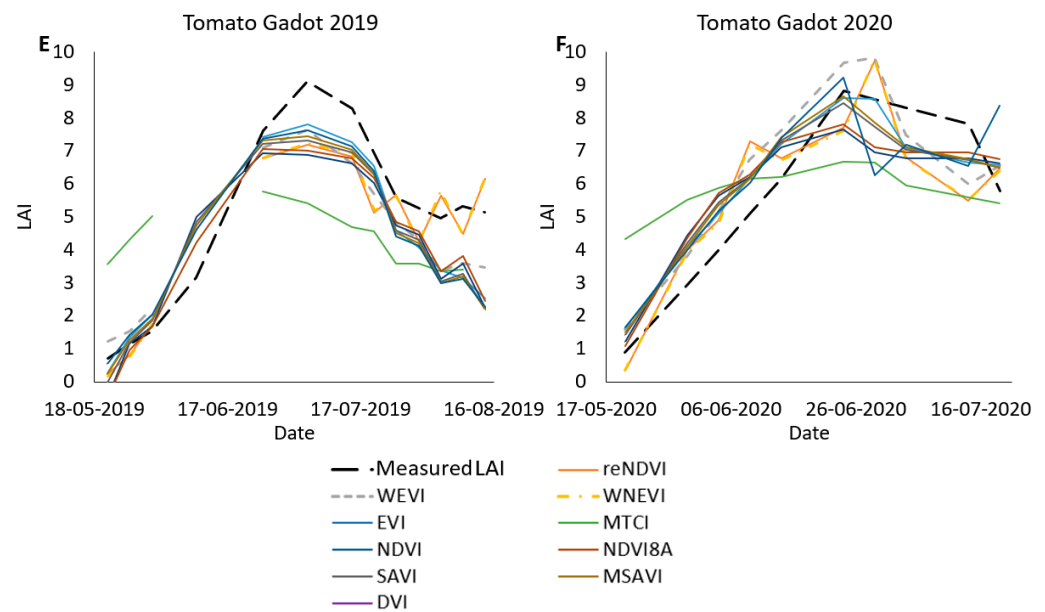


Figure 6. LAI measurements and LAI estimation based on the VIs used in the present study in the following experiments: (A) Wheat Saad, (B) Wheat Yavne, (C) Cotton Megido (centre of the field), (D) Tomato Gadash 2019, (E) Tomato Gadot 2019, (F) Tomato Gadot 2020.

4. Discussion

This study investigated the performance of the individual Sentinel-2 bands and VIs in estimating LAI of tomato, cotton, and wheat. This study's most important finding is that bands 6, 7, 8, 8A, 9 performed well in LAI estimation and did not saturate at high LAI in cotton and processing tomatoes. At the same time, the wheat data was insufficient to make this determination. Therefore, these bands can be used to create VIs for LAI monitoring. VIs such as reNDVI and two new VIs introduced in this study for the first time, WEVI and WNEVI, which are based on these bands, performed well in LAI estimation, better than the commonly used NDVI as well as all the other VIs used in the study.

Band-8A (Narrow NIR) showed better performance in LAI estimation compared to Band-8 (NIR). Therefore, NDVI derived based on Band-8A performed better than NDVI based on Band-8. Band-4 (Red) was found to have an average performance. Therefore, substituting Band-8 with Band-8A and possibly substituting Band-4 with a better-performing band (such as Band-6 used in reNDVI) is likely to improve the correlation of VIs with LAI, and facilitate more accurate agricultural monitoring. The high performance of the reNDVI achieved in the study supported this hypothesis. Unlike red edge and NIR bands, Band-9 (Water vapor) is not commonly used as a VI formulae but can be used in VIs such as WEVI and WNEVI developed in this study. The analysis of Band-9 performance, which is not commonly used for agricultural monitoring, and developing VIs based on this band that perform well in LAI estimation of the three crops, is the unique feature of the present study.

Unlike red edge bands 6 and 7 that showed high performance, Band-5 (Red edge-1), at the tail of the chlorophyll absorption peak [41], showed the lowest overall performance out of all the red edge bands. This might be explained by the negative effect of the chlorophyll content present in the leaves [10,14,42–44], which reaches maximum absorbance at about 690 nm [45]. Moreover, chlorophyll content may vary independently from LAI [46]. In this study, MTCI, based on Band-5, showed low performance in tomato LAI estimation. MTCI was previously found to have low correlation with tomato crop coefficient (K_c) and height [11]. Nevertheless, MTCI was highly correlated with LAI of cotton and wheat in the present study. MTCI was also previously found to have very high correlation with cotton K_c [47,48] as well as a very good correlation with leaf chlorophyll concentration [25,49] and LAI of many crops [3,23,50]. Consequently, despite its effective use for crop variable estimation in many cases, Band-5 and VIs based on this band (e.g., MTCI) should be used

with caution to model tomato variables. Similarly, careful selection of Sentinel-2 bands might improve the performance of various machine learning algorithms, for example, the SNAP Biophysical processor [51].

The results and approach demonstrated in this study can be useful in many agricultural applications based on remote sensing data, for example Zaeen et al., [52] who developed in-season potato yield prediction models based on several VIs, and Kganyago et al., [22] that studied the performance of SNAP Biophysical processor machine learning algorithm in LAI estimation of several crops. These applications might benefit from further investigation of the correlations between Sentinel-2 bands and various vegetation variables.

In the present study, all the Sentinel-2 bands and the majority of VIs (except reNDVI, WEVI, and WNEVI) showed low performance in LAI estimation of wheat. Therefore, despite the achievements in estimating LAI using Sentinel-2 bands in tomato, cotton, and wheat, additional measurements of wheat are needed to estimate Sentinel-2 bands saturation levels in that crop. Moreover, owing to the spectral resemblance of the Sentinel-2 MSI and the VEN μ S sensors [2,11,53], a combination with VEN μ S might facilitate better agricultural monitoring, considering its high two-day temporal resolution.

Overall, the study quantified the performance of the individual Sentinel-2 bands and several VIs (including two newly developed VIs) in the LAI estimation of tomato, cotton, and wheat. Such a result facilitates deriving efficient algorithms and methods for agricultural monitoring via optical satellite imagery.

5. Conclusions

This study is a step towards improving agricultural practices such as variable rate irrigation, fertilizer and herbicide application, yield prediction, disease monitoring, and many others. This achievement is made possible because of the newly-derived VIs and models that can estimate LAI throughout the season without saturation. As a result, agricultural practices informed through remote sensing can potentially improve agricultural production.

This study found that Sentinel-2 Band-8A (Narrow NIR) is more accurate for LAI estimation than Band-8 (NIR). A very important achievement of the study is that the Band-5 (Red edge-1) showed a low correlation with LAI. Band 9 (Water vapour) showed a very high correlation with LAI alongside the red-edge bands 6 and 7 and NIR bands. Band-9 was demonstrated to be effective for LAI estimation when incorporated into new VIs suggested here for the first time, WEVI and WNEVI. Importantly, Bands 1, 2, 3, 4, 5, 11, 12 were saturated at LAI \approx 3 and were practically not responsive to a further increase in LAI around LAI \approx 6. Bands 6, 7, 8, 8A, 9 did not saturate at high LAI. reNDVI, WEVI, and WNEVI were found to be the best performing VIs for LAI estimation of all three crops tested in this study.

Author Contributions: Conceptualisation G.K., O.R.; Methodology, Software, Investigation, G.K.; Writing—original draft preparation, review and editing, Visualisation, G.K., O.R.; Supervision, Project administration, Funding acquisition, O.R. All authors have read and agreed to the published version of the manuscript.

Funding: The field measurements were funded by the Chief Scientist of the Ministry of Agriculture, Israel, under grant 20-21-0006 and by the Ministry of Science and Technology, Israel, under grant numbers 3-14559, 3-15605.

Institutional Review Board Statement: Not applicable.

Informed Consent Statement: Not applicable.

Data Availability Statement: Sentinel-2 data were obtained from the ESA Copernicus Open Access Hub website (<https://scihub.copernicus.eu/dhus/#/home>, accessed on 26 April 2021).

Acknowledgments: We thank Bar Avni-Naor, Nitai Heymann, Lior Fine, Victor Lukyanov, and Nitzan Malachy for their contribution to data processing and fieldwork. We also thank all the growers.

Conflicts of Interest: The authors declare no conflict of interest.

Appendix A

Table A1. Sentinel-2 images inventory and LAI measurements data used in the study.

| | Gadash 2019 | | | Gadot 2019 | | | Gadot 2020 | | | Megido 2020 | | | Saad 2018 | | | Yavne 2019 | | |
|----|----------------------|------------------|-----------|----------------------|------------------|-----------|-------------------|------------------|-----------|----------------------|-----------------------|------------------|-------------------|------------------|-----------|-------------------|------------------|-----------|
| | Tomato | | LAI Value | Tomato | | LAI Value | Tomato | | LAI Value | Cotton | | LAI Value | Wheat | | LAI Value | Wheat | | LAI Value |
| | Sentinel-2 Images | LAI Measurements | LAI Value | Sentinel-2 Images | LAI Measurements | LAI Value | Sentinel-2 Images | LAI Measurements | LAI Value | Sentinel-2 Images | LAI Measurements | LAI Value | Sentinel-2 Images | LAI Measurements | LAI Value | Sentinel-2 Images | LAI Measurements | LAI Value |
| 1 | 21 May | 16 May | 0.6 | 21 May | 16 May | 0.3 | 20 May | 20 May | 0.8 | 30 May ² | 25 May ² | 0.3 ² | 2 March | 1 March | 7.0 | 11 January | 6 January | 3.5 |
| 2 | 26 May | 28 May | 2.5 | 26 May | 28 May | 1.3 | 30 May | 27 May | 2.3 | 4 June ² | 9 June ² | 1.1 ² | 7 March | 14 March | 7.1 | 16 January | 20 February | 6.6 |
| 3 | 31 May | 12 June | 3.0 | 31 May | 4 June | 1.8 | 4 June | 14 June | 6.2 | 9 June ² | 17 June ² | 2.3 ² | 17 March | 25 March | 7.5 | 21 January | 7 March | 7.7 |
| 4 | 10 June ¹ | 27 June | 3.6 | 10 June ¹ | 12 June | 3.6 | 9 June | 24 June | 8.8 | 14 June ² | 2 July ² | 5.3 ² | 22 March | 9 April | 5.0 | 26 January | 21 March | 6.8 |
| 5 | 25 June | 10 July | 3.5 | 25 June | 27 June | 8.2 | 14 June | 14 July | 7.8 | 4 July ²⁰ | 19 July ² | 9.6 ² | 27 March | | | 31 January | 28 March | 7.3 |
| 6 | 5 July | 25 July | 4.7 | 5 July | 3 July | 8.9 | 24 June | 21 July | 5.0 | 14 July ² | 2 August ² | 8.7 ² | 6 April | | | 5 February | 7 April | 6.4 |
| 7 | 15 July | | | 15 July | 10 July | 9.7 | 29 June | | | 19 July ² | | | | | | 25 February | 11 April | 4.4 |
| 8 | 20 July | | | 20 July | 25 July | 5.6 | 4 July | | | 24 July ² | | | | | | | | |
| 9 | 25 July | | | 25 July | 7 August | 4.8 | 14 July | | | 29 July ² | | | | | | | | |
| 10 | | | | 30 July | 11 August | 5.8 | 19 July | | | 30 May ³ | 25 May ³ | 0.6 ³ | | | | | | |
| 11 | | | | 4 August | 15 August | 4.9 | | | | 4 June ³ | 9 June ³ | 1.3 ³ | | | | | | |
| 12 | | | | 9 August | | | | | | 9 June ³ | 17 June ³ | 2.2 ³ | | | | | | |
| 13 | | | | 14 August | | | | | | 14 June ³ | | | | | | | | |

¹ A defective red edge band in a Sentinel-2 image acquired on 10 June 2019 prevented the derivation of red edge-based models for that date. ² Polygon in the centre of the field. ³ NW polygon.

References

- Ewert, F. Modelling plant responses to elevated CO₂: How important is leaf area index? *Ann. Bot.* **2004**, *93*, 619–627. [CrossRef]
- Herrmann, I.; Pimstein, A.; Karnieli, A.; Cohen, Y.; Alchanatis, V.; Bonfil, D.J. LAI assessment of wheat and potato crops by VEN μ S and Sentinel-2 bands. *Remote Sens. Environ.* **2011**, *115*, 2141–2151. [CrossRef]
- Nguy-Robertson, A.L.; Peng, Y.; Gitelson, A.A.; Arkebauer, T.J.; Pimstein, A.; Herrmann, I.; Karnieli, A.; Rundquist, D.C.; Bonfil, D.J. Estimating green LAI in four crops: Potential of determining optimal spectral bands for a universal algorithm. *Agric. For. Meteorol.* **2014**, *192–193*, 140–148. [CrossRef]
- Heuvelink, E.; Bakker, M.J.; Elings, A.; Kaarsemaker, R.; Marcelis, L.F.M. Effect of leaf area on tomato yield. *Acta Hort.* **2005**, *691*, 43–50. [CrossRef]
- Sadeh, Y.; Zhu, X.; Dunkerley, D.; Walker, J.P.; Zhang, Y.; Rozenstein, O.; Manivasagam, V.S.; Chenu, K. Fusion of Sentinel-2 and PlanetScope time-series data into daily 3 m surface reflectance and wheat LAI monitoring. *Int. J. Appl. Earth Obs. Geoinf.* **2021**, *96*, 102260. [CrossRef]
- Manivasagam, V.S.; Rozenstein, O. Practices for upscaling crop simulation models from field scale to large regions. *Comput. Electron. Agric.* **2020**, *175*, 105554. [CrossRef]
- Simic Milas, A.; Romanko, M.; Reil, P.; Abeysinghe, T.; Marambe, A. The importance of leaf area index in mapping chlorophyll content of corn under different agricultural treatments using UAV images. *Int. J. Remote Sens.* **2018**, *39*, 5415–5431. [CrossRef]
- Kang, Y.; Özdoğan, M.; Zipper, S.C.; Román, M.O.; Walker, J.; Hong, S.Y.; Marshall, M.; Magliulo, V.; Moreno, J.; Alonso, L.; et al. How Universal Is the Relationship between Remotely Sensed Vegetation Indices and Crop Leaf Area Index? A Global Assessment. *Remote Sens.* **2016**, *8*, 597. [CrossRef]
- Kamenova, I.; Dimitrov, P. Evaluation of Sentinel-2 vegetation indices for prediction of LAI, fAPAR and fCover of winter wheat in Bulgaria. *Eur. J. Remote Sens.* **2020**, *54*, 89–108. [CrossRef]
- Sener, M.; Arslanoğlu, M.C. Selection of the most suitable Sentinel-2 bands and vegetation index for crop classification by using Artificial Neural Network (ANN) and Google Earth Engine (GEE). *Fresenius Environ. Bull.* **2019**, *28*, 9348–9358.
- Kaplan, G.; Fine, L.; Lukyanov, V.; Manivasagam, V.S.; Malachy, N.; Tanny, J.; Rozenstein, O. Estimating Processing Tomato Water Consumption, Leaf Area Index, and Height Using Sentinel-2 and VEN μ S Imagery. *Remote Sens.* **2021**, *13*, 1046. [CrossRef]
- Asrar, G.; Fuchs, M.; Kanemasu, E.T.; Hatfield, J.L. Estimating Absorbed Photosynthetic Radiation and Leaf Area Index from Spectral Reflectance in Wheat. *Agron. J.* **1984**, *76*, 300. [CrossRef]
- Reichenau, T.G.; Korres, W.; Montzka, C.; Fiener, P.; Wilken, F.; Stadler, A.; Waldhoff, G.; Schneider, K. Spatial heterogeneity of Leaf Area Index (LAI) and its temporal course on arable land: Combining field measurements, remote sensing and simulation in a Comprehensive Data Analysis Approach (CDAA). *PLoS ONE* **2016**, *11*, e0158451. [CrossRef]
- Sun, Y.; Qin, Q.; Ren, H.; Zhang, T.; Chen, S. Red-Edge Band Vegetation Indices for Leaf Area Index Estimation from Sentinel-2/MSI Imagery. *IEEE Trans. Geosci. Remote Sens.* **2020**, *58*, 826–840. [CrossRef]
- Zheng, G.; Moskal, L.M. Retrieving Leaf Area Index (LAI) Using Remote Sensing: Theories, Methods and Sensors. *Sensors* **2009**, *9*, 2719–2745. [CrossRef] [PubMed]
- Xavier, A.C.; Vettorazzi, C.A. Monitoring leaf area index at watershed level through NDVI from Landsat-7/ETM+ data. *Sci. Agric.* **2004**, *61*, 243–252. [CrossRef]
- Ho, P.-G.P. (Ed.) *Geoscience and Remote Sensing*, 1st ed.; InTech: Vukovar, Croatia, 2009; ISBN 978-953-307-003-2.
- Lemoine, G.; Defourny, P.; Gallego, J.; Davidson, A.M.; Fiset, T.; McNairn, H.; Daneshfar, B.; Ray, S.; Neetu; Rojas, O.; et al. *Handbook on Remote Sensing for Agricultural Statistics*; GSARS: Rome, Italy, 2017. Available online: <http://www.fao.org/3/ca6394en/ca6394en.pdf> (accessed on 8 May 2021).
- Horler, D.N.H.; Dockray, M.; Barber, J. The red edge of plant leaf reflectance. *Int. J. Remote Sens.* **1983**, *4*, 273–288. [CrossRef]
- Cui, Z.; Kerekes, J.P. Potential of red edge spectral bands in future landsat satellites on agroecosystem canopy green leaf area index retrieval. *Remote Sens.* **2018**, *10*, 1458. [CrossRef]
- Verrelst, J.; Rivera, J.P.; Veroustraete, F.; Muñoz-Mari, J.; Clevers, J.G.P.W.; Camps-Valls, G.; Moreno, J. Experimental Sentinel-2 LAI estimation using parametric, non-parametric and physical retrieval methods—A comparison. *ISPRS J. Photogramm. Remote Sens.* **2015**, *108*, 260–272. [CrossRef]
- Kganyago, M.; Mhangara, P.; Alexandridis, T.; Laneve, G.; Ovakoglou, G.; Mashiyi, N. Validation of Sentinel-2 leaf area index (LAI) product derived from SNAP toolbox and its comparison with global LAI products in an African semi-arid agricultural landscape. *Remote Sens. Lett.* **2020**, *11*, 883–892. [CrossRef]
- Xie, Q.; Dash, J.; Huete, A.; Jiang, A.; Yin, G.; Ding, Y.; Peng, D.; Hall, C.C.; Brown, L.; Shi, Y.; et al. Retrieval of crop biophysical parameters from Sentinel-2 remote sensing imagery. *Int. J. Appl. Earth Obs. Geoinf.* **2019**, *80*, 187–195. [CrossRef]
- Mutanga, O.; Skidmore, A.K. Narrow band vegetation indices overcome the saturation problem in biomass estimation. *Int. J. Remote Sens.* **2004**, *25*, 3999–4014. [CrossRef]
- Frampton, W.J.; Dash, J.; Watmough, G.; Milton, E.J. Evaluating the capabilities of Sentinel-2 for quantitative estimation of biophysical variables in vegetation. *ISPRS J. Photogramm. Remote Sens.* **2013**, *82*, 83–92. [CrossRef]
- Delegido, J.; Verrelst, J.; Meza, C.M.; Rivera, J.P.; Alonso, L.; Moreno, J. A red-edge spectral index for remote sensing estimation of green LAI over agroecosystems. *Eur. J. Agron.* **2013**, *46*, 42–52. [CrossRef]

27. Reville, A.; Florence, A.; MacArthur, A.; Hoad, S.P.; Rees, R.M.; Williams, M. The value of Sentinel-2 spectral bands for the assessment of winter wheat growth and development. *Remote Sens.* **2019**, *11*, 2050. [CrossRef]
28. Amin, E.; Verrelst, J.; Rivera-Caicedo, J.P.; Pipia, L.; Ruiz-Verdú, A.; Moreno, J. Prototyping Sentinel-2 green LAI and brown LAI products for cropland monitoring. *Remote Sens. Environ.* **2021**, *255*, 112168. [CrossRef]
29. Sun, Y.; Qin, Q.; Ren, H.; Zhang, Y. Decameter Cropland LAI/FPAR Estimation From Sentinel-2 Imagery Using Google Earth Engine. *IEEE Trans. Geosci. Remote Sens.* **2021**. [CrossRef]
30. Beeri, O.; Netzer, Y.; Munitz, S.; Mintz, D.F.; Pelta, R.; Shilo, T.; Horesh, A.; Mey-tal, S. Kc and LAI estimations using optical and SAR remote sensing imagery for vineyards plots. *Remote Sens.* **2020**, *12*, 3478. [CrossRef]
31. Verma, A.; Kumar, A.; Lal, K. Kharif crop characterization using combination of SAR and MSI Optical Sentinel Satellite datasets. *J. Earth Syst. Sci.* **2019**, *128*, 230. [CrossRef]
32. Reville, A.; Florence, A.; MacArthur, A.; Hoad, S.; Rees, R.; Williams, M. Quantifying uncertainty and bridging the scaling gap in the retrieval of leaf area index by coupling Sentinel-2 and UAV observations. *Remote Sens.* **2020**, *12*, 1843. [CrossRef]
33. Louis, J.; Debaecker, V.; Pflug, B.; Main-Knorn, M.; Bieniarz, J.; Mueller-Wilm, U.; Cadau, E.; Gascon, F. Sentinel-2 Sen2cor: L2a processor for users. *Proceedings Living Planet Symposium 2016*. Available online: https://elib.dlr.de/107381/1/LPS2016_sm10_3louis.pdf (accessed on 8 May 2021).
34. Tucker, C.J. Red and photographic infrared linear combinations for monitoring vegetation. *Remote Sens. Environ.* **1979**, *8*, 127–150. [CrossRef]
35. Van Beek, J.; Tits, L.; Somers, B.; Coppin, P. Stem Water Potential Monitoring in Pear Orchards through WorldView-2 Multispectral Imagery. *Remote Sens.* **2013**, *5*, 6647–6666. [CrossRef]
36. Dash, J.; Curran, P.J. Evaluation of the MERIS terrestrial chlorophyll index (MTCI). *Adv. Space Res.* **2007**, *39*, 100–104. [CrossRef]
37. Clevers, J.G.P.W. Application of a weighted infrared-red vegetation index for estimating Leaf Area Index by Correcting for Soil Moisture. *Remote Sens. Environ.* **1989**, *29*, 25–37. [CrossRef]
38. Huete, A.; Didan, K.; Miura, T.; Rodriguez, E.P.; Gao, X.; Ferreira, L.G. Overview of the radiometric and biophysical performance of the MODIS vegetation indices. *Remote Sens. Environ.* **2002**, *83*, 195–213. [CrossRef]
39. Huete, A.R. A soil-adjusted vegetation index (SAVI). *Remote Sens. Environ.* **1988**, *25*, 295–309. [CrossRef]
40. Qi, J.; Chehbouni, A.; Huete, A.R.; Kerr, Y.H.; Sorooshian, S. A modified soil adjusted vegetation index. *Remote Sens. Environ.* **1994**, *48*, 119–126. [CrossRef]
41. Pasqualotto, N.; Delegido, J.; Van Wittenberghe, S.; Rinaldi, M.; Moreno, J. Multi-crop green LAI estimation with a new simple Sentinel-2 LAI index (SeLI). *Sensors* **2019**, *19*, 904. [CrossRef]
42. Meyer, L.H.; Heurich, M.; Beudert, B.; Premier, J.; Pflugmacher, D. Comparison of Landsat-8 and Sentinel-2 data for estimation of leaf area index in temperate forests. *Remote Sens.* **2019**, *11*, 1160. [CrossRef]
43. Xie, Q.; Dash, J.; Huang, W.; Peng, D.; Qin, Q.; Mortimer, H.; Casa, R.; Pignatti, S.; Laneve, G.; Pascucci, S.; et al. Vegetation Indices Combining the Red and Red-Edge Spectral Information for Leaf Area Index Retrieval. *IEEE J. Sel. Top. Appl. Earth Obs. Remote Sens.* **2018**, *11*, 1482–1492. [CrossRef]
44. Clevers, J.; Kooistra, L.; van den Brande, M. Using Sentinel-2 Data for Retrieving LAI and Leaf and Canopy Chlorophyll Content of a Potato Crop. *Remote Sens.* **2017**, *9*, 405. [CrossRef]
45. Lanfri, S. *Vegetation Analysis Using Remote Sensing*; Cordoba National University (UNC): Cordoba, Argentina, 2010.
46. Broge, N.H.; Thomsen, A.G.; Andersen, P.B. Comparison of selected vegetation indices as indicators of crop status. *Geoinf. Eur. Integr.* **2003**, 591–596.
47. Rozenstein, O.; Haymann, N.; Kaplan, G.; Tanny, J. Estimating cotton water consumption using a time series of Sentinel-2 imagery. *Agric. Water Manag.* **2018**, *207*, 44–52. [CrossRef]
48. Rozenstein, O.; Haymann, N.; Kaplan, G.; Tanny, J. Validation of the cotton crop coefficient estimation model based on Sentinel-2 imagery and eddy covariance measurements. *Agric. Water Manag.* **2019**, *223*, 105715. [CrossRef]
49. Clevers, J.G.P.W.; Gitelson, A.A. Remote estimation of crop and grass chlorophyll and nitrogen content using red-edge bands on Sentinel-2 and -3. *Int. J. Appl. Earth Obs. Geoinf.* **2013**, *23*, 344–351. [CrossRef]
50. Viña, A.; Gitelson, A.A.; Nguy-Robertson, A.L.; Peng, Y. Comparison of different vegetation indices for the remote assessment of green leaf area index of crops. *Remote Sens. Environ.* **2011**, *115*, 3468–3478. [CrossRef]
51. Weiss, M.; Baret, F. S2ToolBox Level 2 Products: LAI, FAPAR, FCOVER. Available online: http://step.esa.int/docs/extra/ATBD_S2ToolBox_L2B_V1.1.pdf (accessed on 21 February 2021).
52. Zaeen, A.A.; Sharma, L.; Jasim, A.; Bali, S.; Buzza, A.; Alyokhin, A. In-season potato yield prediction with active optical sensors. *Agrosyst. Geosci. Environ.* **2020**, *3*, e20024. [CrossRef]
53. Manivasagam, V.S.; Kaplan, G.; Rozenstein, O. Developing Transformation Functions for VEN μ S and Sentinel-2 Surface Reflectance over Israel. *Remote Sens.* **2019**, *11*, 1710. [CrossRef]